Highly ordered arrays of macroscopically long Pb nanobelts with atomic-level controlled thickness and width on Si

Z. L. Guan,[1] R. Wu,[1] Y. X. Ning,[1] C. L. Song,[1] L. Tang,[1] D. Hao,[1] Xu-Cun Ma,[1,a)] J. F. Jia,[2] X. Chen,[2] Q. K. Xue,[2,a)] Z. M. Liao,[3] and D. P. Yu[3]
[1]*Institute of Physics, Chinese Academy of Sciences, Beijing 100190, People's Republic of China*
[2]*Department of Physics, Tsinghua University, Beijing 100084, People's Republic of China*
[3]*School of Physics, Peking University, Beijing 100871, People's Republic of China*

(Received 27 April 2008; accepted 14 June 2008; published online 16 July 2008)

We report growth of ordered arrays of superlong Pb nanobelts using Al decorated Si(111) substrates as a template. By depositing Al at substrate temperature of 650–700 °C, each original Si(111) terrace is divided into two distinct strips, a γ-phase strip and a mixed $\sqrt{7}\times\sqrt{7}$ and $\sqrt{3}\times\sqrt{3}$ structure strip. *In situ* scanning tunneling microscopy observation reveals that Pb atoms preferentially nucleate on the γ-phase strips and form uniform array of nanobelts with a width from 10 to 100 nm and a thickness from 2.3 to 20 nm, which can delicately be controlled by Al coverage and Pb coverage. © *2008 American Institute of Physics*. [DOI: 10.1063/1.2955823]

Recently, one-dimensional (1D) metallic nanostructures have attracted considerable attention for their fascinating properties and potential applications in nanoscale devices.[1–6] Various approaches such as nanolithography, vapor-liquid-solid (VLS) growth, and template-directed method were used to fabricate metal nanowire arrays.[7–10] However, the nanowires made by lithography are size limited, and catalysts are incorporated into the wires in VLS, while those obtained by template synthesis are often polycrystalline in nature. More critically, in most cases, the length of nanowires is limited to micrometer scale and precise size control is extremely difficult for long nanowires. Here we report on a simple method to grow arrays of single crystal metal (Pb) nanobelts with atomic-level controlled width and thickness, and with macroscopic length up to centimeter scale of a Si substrate.

The details of the experimental setup and the procedures for clean Si substrate (*n*-type with a resistivity of 0.5 Ω cm) have been described elsewhere.[11] The Al-decorated strip surfaces, which are the template for nanobelt growth, were prepared by depositing Al atoms on Si substrates held at 650 °C. Pb atoms were deposited on the template at low temperature ~150 K, and then the samples were annealed to room temperature (RT) to form nanobelts.

Depending on growth temperature and Al coverage, there exist mainly four reconstructions, α-7×7, $\sqrt{3}\times\sqrt{3}$, $\sqrt{7}\times\sqrt{7}$, and γ-phase in Al/Si(111) system.[12] $\sqrt{3}\times\sqrt{3}$ phase (coverage $\theta_{Al}=\frac{1}{3}$ ML) and $\sqrt{7}\times\sqrt{7}$ phase ($\theta_{Al}=\frac{3}{7}$ ML) often coexist when the growth temperature is between 600 and 700 °C.[12] In the present experiment, the growth temperature was set at 650 °C, more than $\frac{1}{3}$ ML Al (but less than 1 ML for the γ-phase) were deposited. As a result, an unique structure was formed. As shown in Fig. 1(a) and more clearly depicted by the schematic in Fig. 1(b), each Si terrace is divided into two distinct strips; an Al-rich γ-phase strip along the downstairs step edge of the terrace indicated by the black arrows (the original Si steps are pointed out by the blue arrows) and a less Al-rich strip along the upstairs edge with mixed $\sqrt{7}\times\sqrt{7}$ and $\sqrt{3}\times\sqrt{3}$ structure (the red arrows). The high resolution scanning tunnel microscope (STM) images of the γ-phase and the mixed phase are shown in Figs. 1(c) and 1(d), respectively. Due to different electronic structure (the γ-phase is metallic),[13] the apparent height difference between the γ-phase and the mixed phase is 0.14 nm, hence the boundaries between two strips are imaged like "steps" [see Fig. 1(a)]. Intuitively, such type modulated structure should form an ideal template for growing array of 1D nanostructure if certain material can preferentially nucleate on either strip of the two.

To test this idea, we deposited 6 ML Pb on the surface at 150 K. When the samples were warmed up to RT, a highly ordered array of uniform Pb nanobelts is observed [Fig. 1(e)]. A most striking feature is that all the nanobelts have a

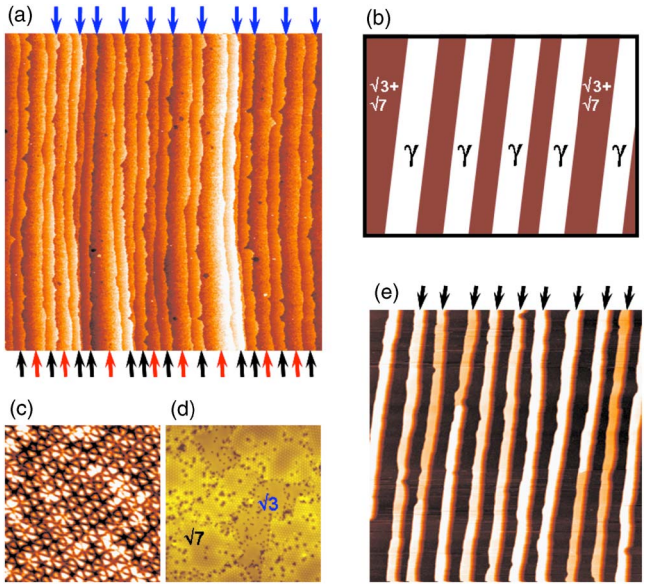

FIG. 1. (Color online) (a) STM image (500×500 nm^2) of the Al-decorated surface formed by 0.48 ML Al deposition on Si. The blue arrows show the original terrace edges, while the black and red arrows the γ-phase strips and the mixed $\sqrt{7}\times\sqrt{7}$ and $\sqrt{3}\times\sqrt{3}$ strips, respectively. High resolution STM image (50×50 nm^2) of (c) the γ-phase surface and (d) the mixed $\sqrt{7}\times\sqrt{7}$ and $\sqrt{3}\times\sqrt{3}$ reconstructions surface. (b) Schematic of phase distribution of the Al-decorated surface. (e) STM image (2000×2000 nm^2) of Pb nanobelt array. The nanobelts are indicated by the black arrows.

[a)]Authors to whom correspondence should be addressed. Electronic addresses: xcma@aphy.iphy.ac.cn and qkxue@mail.tsinghua.edu.cn.

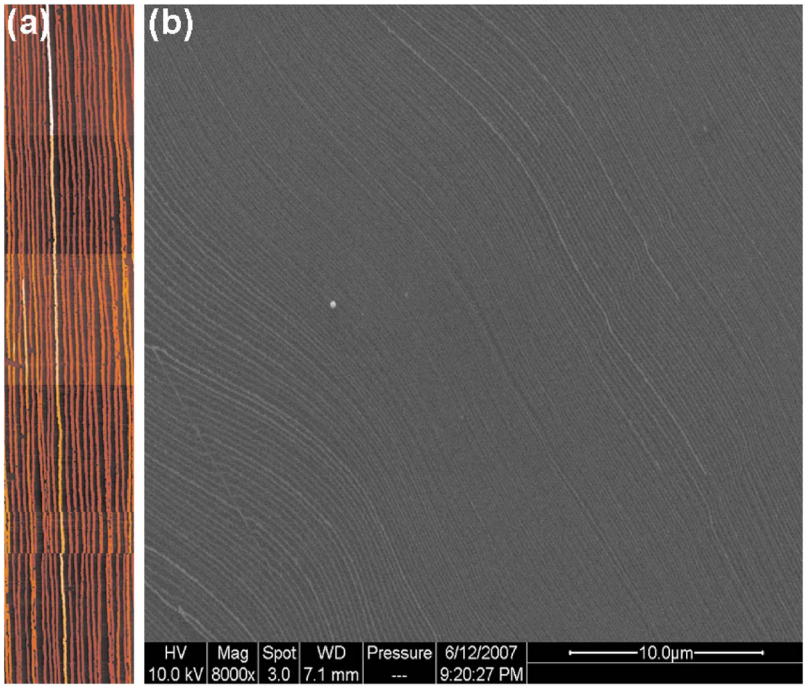

FIG. 2. (Color online) (a) Mosaic STM image (20.8 $\times 4$ μm^2) of Pb nanobelt array. (b) *Ex situ* SEM image (34×29 μm^2) of Pb nanobelt array taken 50 h after the sample growth.

macroscopic length, running all the way of the substrate surface steps. This situation is best illustrated by the large scale mosaic STM image [Fig. 2(a)] and an *ex situ* scanning electron microscope image [Fig. 2(b)].

The black arrows in Fig. 1(e) indicate the location of the γ-phase strips after Pb deposition, suggesting that all the deposited Pb atoms exclusively adsorb on the Al-rich strips to form the nanobelts. Thus, the surface morphology of the nanobelts is essentially a duplication of the Al-rich strip pattern seen in Fig. 1(a). To quantitatively justify it, we carried out an extensive statistical analysis with more than 20 STM images like Fig. 1(e) taken from different surface regions for each Al coverage. In this sample, the average width of Si terraces is 180 nm, which is determined by the cutting angle (0.1°) of Si wafer. The results are summarized in Fig. 3(a). When Al coverage is 0.48 ML, the average width of the γ-phase strips is 83 ± 11 nm, it changes to 70 ± 12 nm at 0.456 ML and to 50 ± 10 nm at 0.43 ML. The average width of the resulted nanobelts is 82 ± 13, 71 ± 11, and 53 ± 10 nm, respectively. Using another Si wafer with a cutting angle of 0.15°, when θ_{Al} is 0.456 ML, the width of the strips and the belts is 45 ± 10, and 43 ± 10 nm, respectively. The template effect is very obvious.

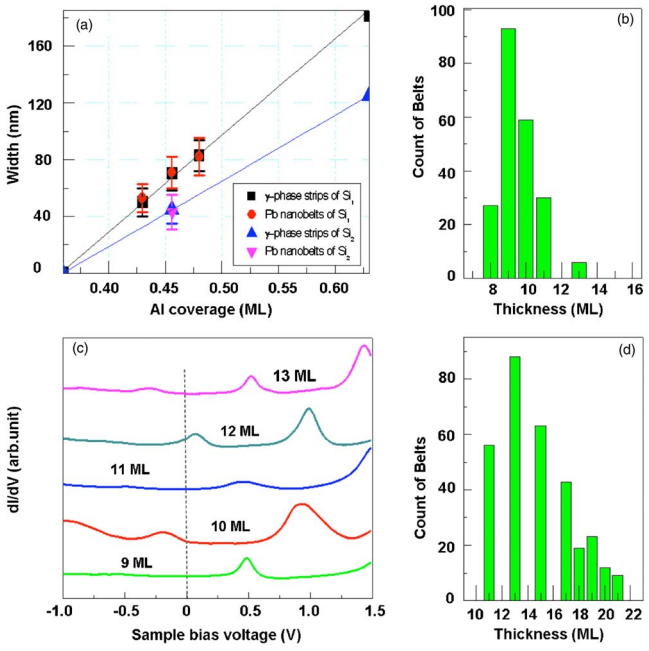

FIG. 3. (Color online) (a) The width of the γ-phase strips as a function of Al coverage. Two different Si wafers with a cutting angle of 0.1° (Si_1) and 0.15° (Si_2) were used. The corresponding average terrace width is 180 nm (Si_1) and 125 nm (Si_2). Height histograms of Pb nanobelts grown by depositing (b) 4 ML and (d) 6 ML Pb on the Al-decorated surface (θ_{Al}=0.48 ML). The average height of Pb nanobelts is 9.6 ML in (b) and 15 ML in (d). (c) dI/dV spectra of Pb nanobelts. The dI/dV curve was measured at 4.32 K by placing a STM tip ~0.6 nm above the Pb belts with standard scanning tunneling spectroscopy technique. The bias modulation is 20 mV_{rms}, and the modulation frequency is 2 kHz.

Under the present growth conditions, we found that the critical Al coverage for preparation of this characteristic strip surface is between 0.36 and 0.63 ML, and that there is a linear dependence of width of the γ-phase strips on the Al coverage [the black line in Fig. 3(a)]. At 0.36 ML, the γ-phase starts nucleation at the step edges, since step edges are the place where Si atoms needed for formation of the γ-phase can easily be supplied,[12] which explains why the γ-phase always appears along the downstairs step edge of a terrace. On the other hand, when Al coverage exceeds 0.63 ML, the terraces will be fully covered by the γ-phase, the striped template disappears. As long as Al coverage falls into this range, the widths of nanobelts can be simply and delicately adjusted by the amount of Al. As for the slope of the black line shown in Fig. 3(a), the experiment reveals that it is determined by the average terrace width of the Si wafers, suggesting that one can tune the separation of nanobelts simply by choosing Si wafers of different orientation.

For certain width of the Al strips and thus the nanobelts, the thickness of nanobelts can conveniently be tuned by Pb coverage. When Pb coverage is 4 ML, the average thickness is 9.6 ± 2 ML [Fig. 3(b)], and it changes to 15 ± 5 ML at θ_{Pb}=6 ML [Fig. 3(d)]. We found that the critical thickness is 8 ML (2.3 nm), the smallest thickness we could prepared at

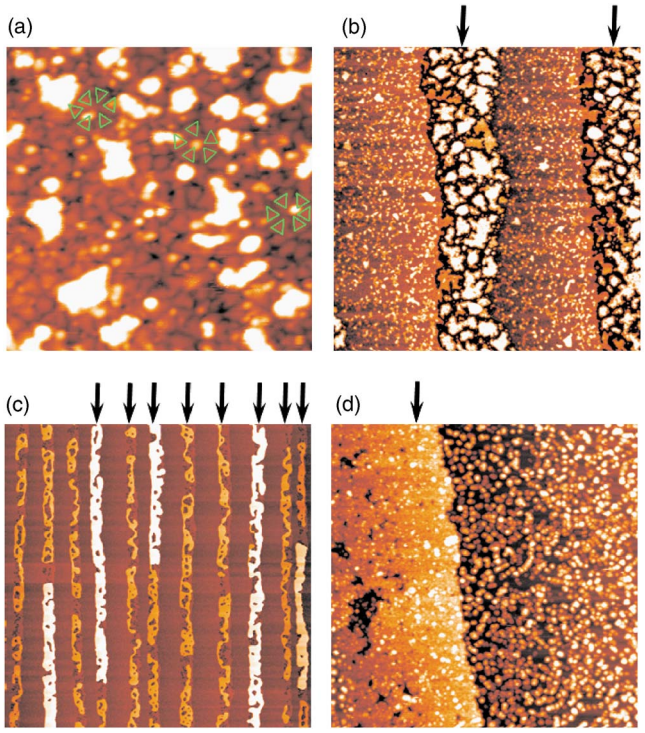

FIG. 4. (Color online) [(a)–(c)] STM images for (a) 0.1 ML, (b) 0.5 ML, and (c) 2 ML Pb deposited on the Al-decorated surface. (d) The wetting layer in (c). The green triangles in (a) indicate the subunits of the γ-phase surface, and the black arrows in [(b)–(d)] the location of the γ-phase strips after Pb deposition. Image size is (a) 50×50 nm^2, (b) 300×300 nm^2, (c) 2000×2000 nm^2, and (d) 200×200 nm^2.

RT, which is previously understood with the so-called "electronic growth model."[14] This method can work for a thickness up to 65 ML (>18 nm). In this case, a trick is that one has to deposit Pb atoms for several times (<8 ML each time). Otherwise, Pb films will be formed. Note that only odd-number layered Pb nanobelts are obtained between 10 and 17 ML [Fig. 3(d)]. The spectra in Fig. 3(c) demonstrate that this preferential thickness is a result of quantum size effects (QSE).[15–17] Due to strong QSE, in thickness range from 8 to 17 ML, odd numbers are favored. However, as shown in Fig. 3(b), there are fewer belts at 11 ML than that at 10 ML. This is because the total surface Pb coverage (4 ML) is not sufficient, and the growth of 11 ML belts just starts.

Next, we discuss why the nanobelts preferentially form on top of the γ-phase. The γ-phase surface shows up as a quasiperiodic incommensurate domain structure.[18] According to previous studies, these domain walls incline to promote the nucleation density.[19,20] In the present experiment, stable Pb nuclei are preferentially (even exclusively) formed on the γ-phase and at corners of the triangular subunits, as shown in Fig. 4(a), which then grow in size and form islands [Fig. 4(b)] and finally nanobelts [Fig. 4(c)]. While on the $\sqrt{3}\times\sqrt{3}$ reconstructions surface, it is difficult for Pb atoms to nucleate, since $\sqrt{3}\times\sqrt{3}$ is stable and there is no dangling bond.[13] Strain is another possible factor for the selective growth in terms of the lattice mismatch (~57.3%) between $\sqrt{3}\times\sqrt{3}$ and Pb(111). Three-dimensional clusters form in this case [the right half of Fig. 4(d)]. On the other hand, the domain structure of the γ-phase could accommodate the strain delicately. As a result, a pseudomorphic smooth Pb wetting layer of 2 ML high was formed [the left half of Fig. 4(d)].

In summary, highly ordered Pb nanobelt arrays have been prepared by using Al-decorated surfaces as a template. The width and thickness of Pb nanobelts could delicately be controlled by Al and Pb coverage, respectively, for certain orientation of the Si wafer at choice. With further deposition of a different metal on the nanobelt array, one can even grow lateral superlattices. More importantly, the macroscopic length makes it very easy to perform measurement of transport properties and fabricate devices on Si chips.

This work is financially supported by the National Natural Science Foundation and the Ministry of Science and Technology of China.

[1] J. T. Hu, M. Ouyang, P. Yang, and C. M. Lieber, Nature (London) **399**, 48 (1999).
[2] A. M. Morales and C. M. Lieber, Science **279**, 208 (1998).
[3] R. C. Ashoori, Nature (London) **379**, 413 (1996).
[4] A. P. Alivisatos, Science **271**, 933 (1996).
[5] S. Iijima, Nature (London) **354**, 56 (1991).
[6] C. Burda, X. B. Chen, R. Narayanan, and M. A. El-Sayed, Chem. Rev. (Washington, D.C.) **105**, 1025 (2005).
[7] A. Bezryadin, C. N. Lau, and M. Tinkham, Nature (London) **404**, 971 (2000).
[8] X. Duan and C. M. Lieber, Adv. Mater. (Weinheim, Ger.) **12**, 298 (2000).
[9] T. M. Whitney, P. C. Searson, J. S. Jiang, and C. L. Chien, Science **261**, 1316 (1993).
[10] C. R. Martin, Science **266**, 1961 (1994).
[11] J. L. Li, J. F. Jia, X. J. Liang, X. Liu, J. Z. Wang, Q. K. Xue, Z. Q. Li, J. S. Tse, Z. Zhang, and S. B. Zhang, Phys. Rev. Lett. **88**, 066101 (2002).
[12] T. Michely, M. C. Reuter, and R. M. Tromp, Phys. Rev. B **53**, 4105 (1996).
[13] R. J. Hamers, Phys. Rev. B **40**, 1657 (1989).
[14] Z. Y. Zhang, Q. Niu, and C. K. Shih, Phys. Rev. Lett. **80**, 5381 (1998).
[15] Y. Guo, Y. F. Zhang, X. Y. Bao, T. Z. Han, Z. Tang, L. X. Zhang, W. G. Zhu, E. G. Wang, Q. Niu, Z. Q. Qiu, J. F. Jia, Z. X. Zhao, and Q. K. Xue, Science **306**, 1915 (2004).
[16] Y. F. Zhang, J. F. Jia, Z. Tang, T. Z. Han, and Q. K. Xue, Surf. Sci. **596**, L331 (2005).
[17] Y. Qi, X. C. Ma, P. Jiang, S. H. Ji, Y. S. Fu, J. F. Jia, Q. K. Xue, and S. B. Zhang, Appl. Phys. Lett. **90**, 013109 (2007).
[18] A. A. Saranin, V. G. Kotlyar, A. V. Zotov, T. V. Kasyanova, M. A. Cherevik, and V. G. Lifshits, Surf. Sci. **517**, 151 (2002).
[19] H. Brune, M. Giovannini, K. Bromann, and K. Kern, Nature (London) **394**, 451 (1998).
[20] T. Michely, M. Hohage, S. Esch, and G. Cosma, Surf. Sci. **349**, L89 (1996).